J. Fluid Mech. (1996), *vol.* 316, *pp.* 325–334

Horizontal fractionation of rising and sinking particles in wind-affected currents

By RONALD SMITH

Mathematical Sciences, Loughborough University, LE11 3TU, UK

(Received 10 July 1995 and in revised form 27 December 1995)

The different rise or sinking velocity for different sizes or types of particles gives different vertical sampling of a wind-affected shallow-water flow. This paper derives a mathematical model for the consequent horizontal fractionation of a dilute suspension of particles when the flow is a wind-influenced perturbation from the classical logarithmic open-channel flow. Simple approximations are given for the effective horizontal velocity and for the shear dispersion tensor which preserve the perfect duality between the sensitivity of sinking particles to bed stress and the sensitivity of rising particles to surface stress.

1. Introduction

As the size of industries and the populations of cities increase, issues of pollution become more and more serious. Much of the pollution is disposed of into lakes, rivers or coastal waters. Some pollutants (e.g. highly radioactive actinides) attach to particulate matter already present in the water. Other pollutants (e.g. sewage sludge) are already in particulate form. An important facet of the understanding and prediction of water pollution levels is to quantify any fractionation of the different particles (see figure 1).

For open-channel flow with a (quasi-turbulent) logarithmic velocity profile, Sumer (1974) and Smith (1986) calculated how the sinking velocity of particles reduces the effective longitudinal speed and increases the longitudinal dispersion of the particles. For a parabolic velocity (quasi-laminar) flow model Smith (1991) quantified the role of wind in the two-dimensional horizontal fractionation. The purpose of this paper is to present the unexpectedly neat results for a logarithmic velocity profile. For the particle movement and spreading there is perfect duality between the sensitivity of sinking particles to bed stress and the sensitivity of rising particles to surface stress.

2. Equations and boundary conditions

For simplicity, we shall focus upon particles of small size and discharges of modest buoyancy input for which the flow, turbulence and biochemical decay rates can be regarded as being given. No allowance is made for any modification by individual particles to the local structure of the turbulence, nor for changes by the overall weight of particles to the global structure of the flow (Dyer & Soulsby 1988). Also, we shall assume that the bed is locally flat ($z = -h$) and that any time dependence takes place more slowly than vertical mixing. The water velocity is represented as

$$(u(z),\ v(z),\ 0). \tag{2.1}$$

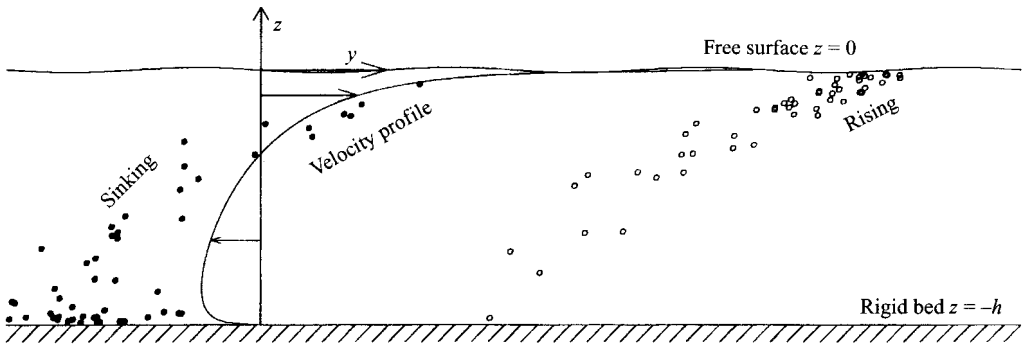

FIGURE 1. Fractionation of rising and sinking particles in wind drift.

The particles are categorized in terms of the rise velocity W relative to the water. The turbulent mixing process is modelled in terms of eddy diffusivities with components $\kappa_1(z)$, $\kappa_2(z)$, $\kappa_3(z)$ in the x, y, z coordinate directions. Biochemical decay $\alpha(z)$ can be related to the penetration of sunlight. The particle release rate in the fluid is denoted $q(x, y, z, t)$. On the free surface there is zero flux of particles, while at the bed the settling flux is assumed to be proportional to the particle concentration. Thus, the particle concentration or mass fraction $c(x, y, z, t)$ is assumed to satisfy the equations and boundary conditions:

$$\partial_t c + \alpha c + u\partial_x c + v\partial_y c + W\partial_z c - \kappa_1\partial_x^2 c - \kappa_2\partial_y^2 c - \partial_z(\kappa_3\partial_z c) = q, \tag{2.2a}$$

with

$$Wc - \kappa_3\partial_z c = 0 \quad \text{on} \quad z = 0, \tag{2.2b}$$

and

$$\kappa_3\partial_z c - Wc = \beta c + q^{(-)} \quad \text{on} \quad z = -h. \tag{2.2c}$$

The settling coefficient β ranges from zero (non-absorbing) to infinity (totally absorbing). The bed source $q^{(-)}$ allows for resuspension of previously settled material. Empirical formulae for the pick-up function $q^{(-)}$ in terms of material and flow parameters are reviewed in van Rijn (1984).

In the important special case of turbulent open-channel flow, correct to order $\eta^{(-)}$, the velocity profile is logarithmic (as illustrated in figure 1) and the vertical eddy diffusivity is parabolic:

$$u(z) = \bar{u}\{1 + \varepsilon[1 + \ln\eta]\} - \frac{\tau_1}{ku_*}\{\varepsilon[1 + \ln\eta] + [1 + \ln(1-\eta)]\}, \tag{2.3a}$$

$$v(z) = \bar{v}\{1 + \varepsilon[1 + \ln\eta]\} - \frac{\tau_2}{ku_*}\{\varepsilon[1 + \ln\eta] + [1 + \ln(1-\eta)]\}, \tag{2.3b}$$

$$\kappa_3(z) = khu_*\eta(1-\eta), \tag{2.3c}$$

with

$$\eta = \eta^{(-)} + \left(1 + \frac{z}{h}\right)(1 - \eta^{(-)} - \eta^{(+)}), \tag{2.3d}$$

$$\varepsilon = \frac{1}{-\ln\eta^{(-)} - 1}, \tag{2.3e}$$

$$u_*^4 = \varepsilon^2(k\bar{u}u_* - \tau_1)^2 + \varepsilon^2(k\bar{v}u_* - \tau_2)^2 + \tau_1^2 + \tau_2^2. \tag{2.3f}$$

Here $(\bar{u}, \bar{v})$ is the vertically averaged velocity, $(\rho\tau_1, \rho\tau_2)$ is the surface wind stress, u_* is a

turbulence velocity scale, k is von Kármán's constant (about 0.4), $\eta^{(-)}$ a dimensionless bed roughness and $\eta^{(+)}$ a dimensionless surface roughness. Both $\eta^{(-)}$ and $\eta^{(+)}$ are exceedingly small (about 0.001). The definition (2.3*e*) of the small parameter ε (about 1/6) ensures that, correct to order $\eta^{(-)}$, the velocities are zero at the bed.

As is suggested by the u_* notation, in the absence of wind the turbulence velocity scale u_* is the usual friction velocity $\varepsilon k(\bar{u}^2 + \bar{v}^2)^{1/2}$. The right-hand side of equation (2.3*f*) is the sum of the squares of stresses at the bed and at the surface, so gives equal importance to turbulence generation at both sites. For small ε^2 but arbitrary sized other terms, a uniformly valid approximation for u_* is

$$u_* = \left\{ \tfrac{1}{2} \left[4(\tau_1^2 + \tau_2^2)(1 + \varepsilon^2) + \varepsilon^4 k^4 (\bar{u}^2 + \bar{v}^2)^2 \right]^{1/2} + \tfrac{1}{2} \varepsilon^2 k^2 (\bar{u}^2 + \bar{v}^2) \right\}^{1/2} - \frac{\varepsilon^2 k(\bar{u}\tau_1 + \bar{v}\tau_2)}{2 \left[4(\tau_1^2 + \tau_2^2)(1 + \varepsilon^2) + \varepsilon^4 k^4 (\bar{u}^2 + \bar{v}^2)^2 \right]^{1/2}}. \tag{2.4}$$

To take a more complete account of the effect of wind, additional equations would be needed to allow for symmetry breaking in the wind-driven contribution to the velocity profile (2.3*a*, *b*), in the turbulence structure (2.3*c*) and in the turbulence magnitude (2.3*f*).

3. Allowing for sinking of particles

In the absence of settling at the bed ($\beta = 0$) there is an equilibrium concentration profile $\gamma(z)$ (normalized to have vertical average $\bar{\gamma} = 1$) in which there is a balance between upwards rise W and vertical mixing κ_3. For turbulent flow with the parabolic eddy diffusivity distribution (2.3*c*), Rouse (1937) derived the power-law concentration profile

$$\gamma(\eta; P) = \frac{\sin \pi P}{\pi P} \left[\frac{\eta}{1 - \eta} \right]^P, \quad \text{with } P = \frac{W}{k u_*}. \tag{3.1a, b}$$

Rising particles tend to have greater concentration near the free surface while sinking particles have greater concentration near the bed (see figures 1 and 2). For P less than -1 the particles are too heavy to remain in suspension. Conversely, for P greater than $+1$ the particles are too buoyant to remain in suspension. At different times or places, gradual variations in u_* would cause variations in the vertical profile of particles with a given rise velocity W.

Although experiments conducted by Coleman (1970) extend well below $P = -1$ and suggest that κ_3 does not tend to zero at the free surface, he shows that the parabolic diffusivity (2.3*c*) does give a reasonable fit to the widely scattered experimental data. Dyer & Soulsby (1988, figures 8, 9, 10) illustrate that several alternative models yield closely similar results for the mass of sediment transported and for the drag at the bed. As is further elaborated here, the model (2.3*a–f*) has the advantage of exact solutions.

In the context of a chromatographic technique known as field flow fractionation, Giddings (1968) exploited the fact that (in the absence of settling) the non-solute character, embodied in the rise velocity W, can be factored out via the reference profile γ:

$$c(x, y, z, t) = \gamma(z) m(x, y, z, t). \tag{3.2}$$

The field equation satisfied by m is as if there were a horizontal velocity $(\gamma u, \gamma v)$ and eddy diffusivities $\gamma\kappa_1$, $\gamma\kappa_2$, $\gamma\kappa_3$ i.e. equation (2.2*a*) with modified coefficients. In the

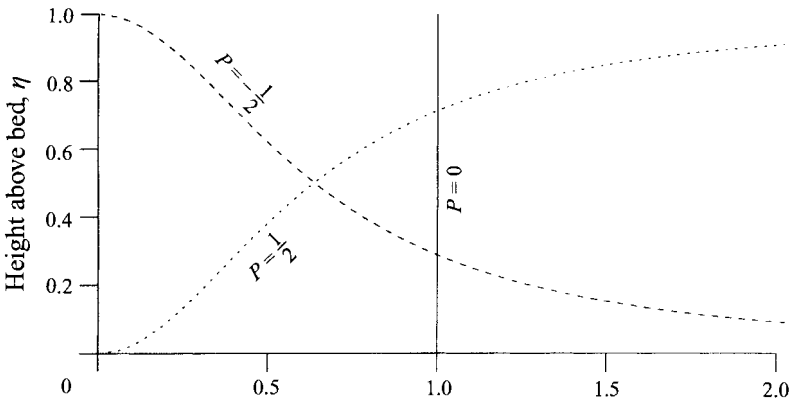

FIGURE 2. Rouse (1937) concentration profiles γ.

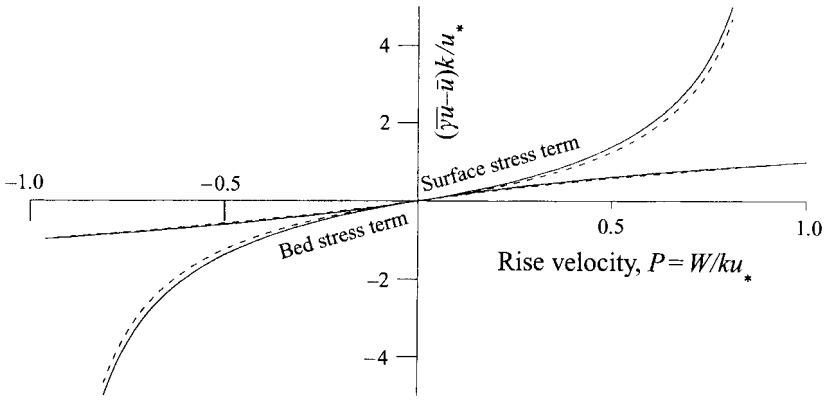

FIGURE 3. Difference in velocity between solute and particles. The dashed curves give the simple approximation (3.4).

absence of settling at the bed, $m(x, y, z, t)$ eventually becomes vertically uniform and is carried along at the horizontal velocity $(\overline{\gamma u}, \overline{\gamma v})$.

For turbulent open-channel flow without wind the e-folding distance for vertical mixing is $1.25h(\bar{u}/u_*)$, i.e. the bulk speed $\bar{u}$ divided by the temporal mixing rate λ_1 (Smith 1986, equation 7.2c). Sumer (1974, equation 35) gives a formula for $\overline{\gamma u}$ involving the psi (digamma) function Ψ. The extension to include wind is

$$\overline{\gamma u} = \bar{u} + \varepsilon\left(\frac{k\bar{u}u_* - \tau_1}{ku_*}\right)[1 + \Psi(1+P) - \Psi(2)] - \frac{\tau_1}{ku_*}[1 + \Psi(1-P) - \Psi(2)]. \quad (3.3)$$

There is up–down duality between the bed stress and surface stress terms. To a reasonable degree of accuracy (see figure 3) we can use the empirical approximation

$$(\overline{\gamma u} - \bar{u})\frac{k}{u_*} = \varepsilon\left(\frac{k\bar{u}u_* - \tau_1}{u_*^2}\right)\frac{P(3+P)}{2(1+P)} + \left(\frac{\tau_1}{u_*^2}\right)\frac{P(3-P)}{2(1-P)}. \quad (3.4)$$

Rising particles (P positive) move faster than $\bar{u}$ and with the wind, while sinking particles (P negative) travel more slowly than $\bar{u}$ and against the wind.

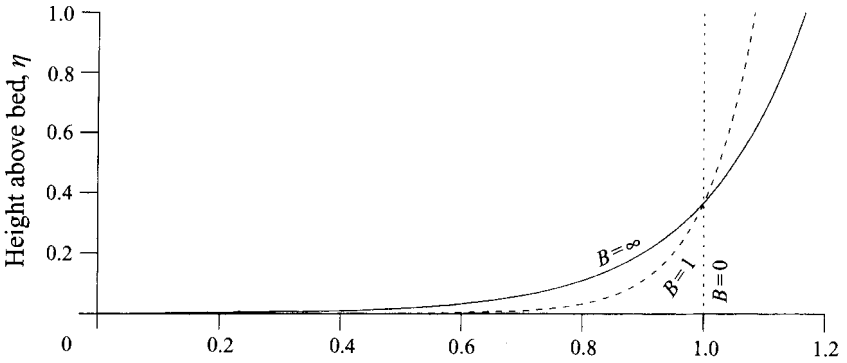

FIGURE 4. Modification ψ_0 to the concentration profile because of settling at the bed. The effective discharge strength is scaled by this same function.

4. Allowing for settling at the bed

The extra complication of settling at the bed ($\beta \neq 0$) is analogous to heat transfer (Sankarasubramanian & Gill 1973; Lungu & Moffatt 1982). There is an additional exponential decay rate λ_0 and an adjustment $\psi_0(z)$ in the shape of the equilibrium concentration profile (normalized to have $\overline{\gamma\psi_0^2} = 1$). For turbulent open-channel flow, with ε small, the near vanishing of κ_3 towards the bed allows the possibility of a boundary-layer type of correction (Smith 1986, §6) similar to that of the velocity profile (see figure 4) with a decay rate λ_0 proportional to the drag:

$$\psi_0 = \frac{1}{1+B} + \frac{B}{1+B}\{1 + \varepsilon[\Psi(2) - \Psi(1+P) + \ln\eta]\} + \ldots, \tag{4.1a}$$

$$\lambda_0 = \frac{u_*^2 B}{h\bar{u}(1+B)} + \ldots \text{ with } B = \frac{\beta\bar{u}}{u_*^2}. \tag{4.1b,c}$$

The parameter B is a non-dimensional measure of the probability that a particle which reaches the bed becomes permanently attached to the bed. In the limit of total retention (B tends to infinity) the exponential decay rate λ_0 corresponds to a downstream distance $h(\bar{u}/u_*)^2$. This is much further than the e-folding distance for vertical mixing. Thus, if settling at the bed is important then the length or time scales are long enough that there will have been thorough vertical mixing.

By analogy with the Giddings (1968) factorization (3.3), we write

$$c(x,y,z,t) = \gamma(z)\psi_0(z)b(x,y,z,t). \tag{4.2}$$

The field equation satisfied by the variable b is as if in equation (2.2a) there were a horizontal velocity $(\gamma\psi_0^2 u, \gamma\psi_0^2 v)$ and eddy diffusivities $\gamma\psi_0^2\kappa_1$, $\gamma\psi_0^2\kappa_2$, $\gamma\psi_0^2\kappa_3$. The complications of vertical drift and bed absorption are accounted for in the $\gamma\psi_0^2$ factors. The notable change (Barton 1984) is that the effective source strengths in the fluid and at the bed are the products $\psi_0 q$ and $\psi_0^{(-)}q^{(-)}$ where the minus superscripts indicate values at the bed. Hence, there is permanent sensitivity to the height of release. In the limiting case β tends to infinity, particles discharged near to the bed would settle immediately and the effective source strength would be zero.

We remark that to leading order in ε the weight factor ψ_0^2 does not change the

effective longitudinal velocity $\overline{\gamma\psi_0^2 u}$. So, equation (3.4) or figure 3 remain applicable whether or not there is settling.

5. Shear dispersion

For solutes the theory of shear dispersion is long established (Taylor 1953; Elder 1959). After vertical mixing of $b(x, y, z, t)$ has been achieved, the weighted concentration

$$c_0(x, y, t) = \overline{\psi_0 c} \tag{5.1}$$

satisfies the two-dimensional advection diffusion equation:

$$\partial_t c_0 + [\overline{\gamma\psi_0^2\alpha} + \lambda_0]c_0 + \overline{\gamma\psi_0^2 u}\partial_x c_0 + \overline{\gamma\psi_0^2 v}\partial_y c_0 - \left[D_{11} + \overline{\gamma\psi_0^2\kappa_1}\right]\partial_x^2 c_0$$

$$-2D_{12}\partial_x\partial_y c_0 - \left[D_{22} + \overline{\gamma\psi_0^2\kappa_2}\right]\partial_y^2 c_0 = \overline{\psi_0 q} + \psi_0^{(-)} q^{(-)}. \tag{5.2}$$

The shear dispersion coefficients D_{11}, D_{12}, D_{22} can be written as integrals of the velocity profiles:

$$D_{11} = \frac{1}{h}\int_{-h}^{0} \frac{1}{\gamma\psi_0^2\kappa_3} \left[\int_{-h}^{z} \gamma\psi_0^2 \left(u - \overline{\gamma\psi_0^2 u}\right) \mathrm{d}z'\right]^2 \mathrm{d}z, \tag{5.3a}$$

$$D_{12} = \frac{1}{h}\int_{-h}^{0} \frac{1}{\gamma\psi_0^2\kappa_3} \left[\int_{-h}^{z} \gamma\psi_0^2 \left(u - \overline{\gamma\psi_0^2 u}\right) \mathrm{d}z'\right] \left[\int_{-h}^{z} \gamma\psi_0^2 \left(v - \overline{\gamma\psi_0^2 v}\right) \mathrm{d}z'\right] \mathrm{d}z, \tag{5.3b}$$

$$D_{22} = \frac{1}{h}\int_{-h}^{0} \frac{1}{\gamma\psi_0^2\kappa_3} \left[\int_{-h}^{z} \gamma\psi_0^2 \left(v - \overline{\gamma\psi_0^2 v}\right) \mathrm{d}z'\right]^2 \mathrm{d}z. \tag{5.3c}$$

For parabolic wind-affected velocity profiles and constant vertical eddy diffusivity Smith (1991, equations (7.3), (7.4)) evaluated these integrals numerically.

For a uni-directional turbulent open-channel flow without wind ($\tau_1 = 0$) and without bed absorption ($B = 0$), Smith (1986) derived a series formula for the shear dispersion coefficient D_{11}. Grouping bed and surface stress terms separately, we write the two-dimensional and wind-driven generalization:

$$\frac{D_{11}k^3}{hu_*} = \varepsilon^2\left(\frac{k\bar{u}u_* - \tau_1}{u_*^2}\right)^2 a_B + 2\varepsilon\left(\frac{k\bar{u}u_* - \tau_1}{u_*^2}\right)\frac{\tau_1}{u_*^2}a_M + \left(\frac{\tau_1}{u_*^2}\right)^2 a_W, \tag{5.4a}$$

$$\frac{D_{12}k^3}{hu_*} = \varepsilon^2\left(\frac{k\bar{u}u_* - \tau_1}{u_*^2}\right)\left(\frac{k\bar{v}u_* - \tau_2}{u_*^2}\right)a_B + \varepsilon\left\{\left(\frac{k\bar{u}u_* - \tau_1}{u_*}\right)\frac{\tau_2}{u_*^2} + \frac{\tau_1}{u_*^2}\left(\frac{k\bar{v}u_* - \tau_2}{u_*}\right)\right\}a_M$$

$$+ \left(\frac{\tau_1}{u_*^2}\right)\left(\frac{\tau_2}{u_*^2}\right)a_W, \tag{5.4b}$$

$$\frac{D_{22}k^3}{hu_*} = \varepsilon^2\left(\frac{k\bar{v}u_* - \tau_2}{u_*^2}\right)^2 a_B + 2\varepsilon\left(\frac{k\bar{v}u_* - \tau_2}{u_*^2}\right)\frac{\tau_2}{u_*^2}a_M + \left(\frac{\tau_2}{u_*^2}\right)^2 a_W. \tag{5.4c}$$

The explicit formulae for the bed stress, mixed and surface stress coefficients are

$$a_B(P) = \sum_{m=1}^{\infty} \frac{(2m+1)}{m^3(m+1)^3} \prod_{j=1}^{m}\left[\frac{1 - P/j}{1 + P/j}\right], \tag{5.5a}$$

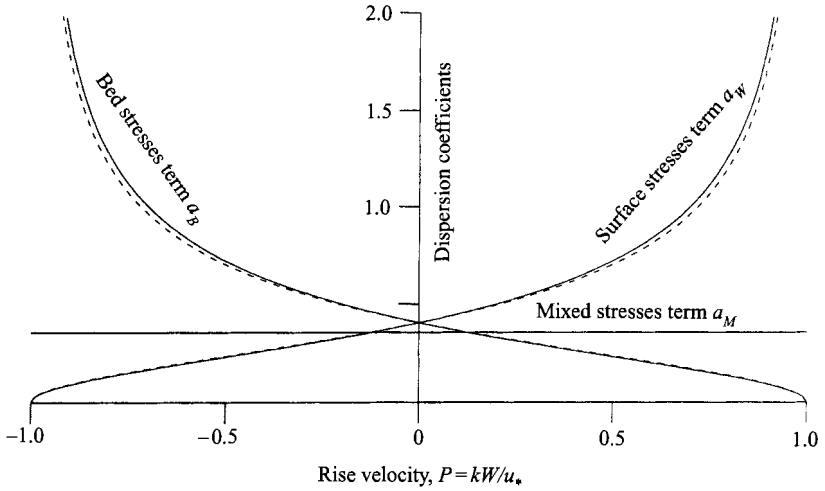

FIGURE 5. Dispersion coefficients for joint wind and bulk flow. The dashed curves give the approximation (5.6).

$$a_M = \sum_{m=1}^{\infty} \frac{(-1)^{m+1}(2m+1)}{m^3(m+1)^3} = 2 - \frac{\pi^2}{6} = 0.35506, \tag{5.5b}$$

$$a_W(P) = a_B(-P) = \sum_{m=1}^{\infty} \frac{(2m+1)}{m^3(m+1)^3} \prod_{j=1}^{m} \left[\frac{1+P/j}{1-P/j}\right]. \tag{5.5c}$$

An empirical approximation (see figure 5) for the P-dependent coefficients $a_B(P)$, $a_W(P)$ is

$$a_B(P) = a_W(-P) = 0.40411 \left[\frac{1-P}{1+P}\right]^{1/2}. \tag{5.6}$$

For the bed stress contribution to the current, the shear is greatest near the bed and consequently the shear dispersion is greatest for sinking particles. For the surface stress contribution to the current (see figure 1) the shear is greatest near the free surface and the shear dispersion is greatest for rising particles (Smith 1991). Remarkably, with the simple flow model used here, there is perfect up–down duality beginning with the eddy viscosity (2.3*d*) and cumulating with the dispersion coefficients (5.5*c*), (5.6).

For the direct turbulence contributions to the horizontal dilution Fischer (1973) suggested the formula

$$\kappa_1 = \kappa_2 = 0.2hu_*\eta^{1/3}. \tag{5.7}$$

Exact and empirical formulae for the required weighted integrals are

$$\overline{\gamma\kappa_1} = \overline{\gamma\kappa_2} = 0.15hu_* \frac{\Gamma(\frac{4}{3}+P)}{\Gamma(\frac{4}{3})\Gamma(1+P)} \sim 0.3hu_* \left(\frac{1+P}{2+P}\right). \tag{5.8}$$

As was noted in the case $P = 0$ by Elder (1959), the longitudinal shear dispersion coefficients (5.4*a–c*) are typically a factor $k^{-4} = 39$ larger than the direct turbulence contribution (5.8). Also, we can estimate that it only requires a cross-flow wind stress of order $k^2u_*^2$ (i.e. about one sixth of the bottom stress) for the cross-flow shear dispersion to be comparable with the turbulent mixing.

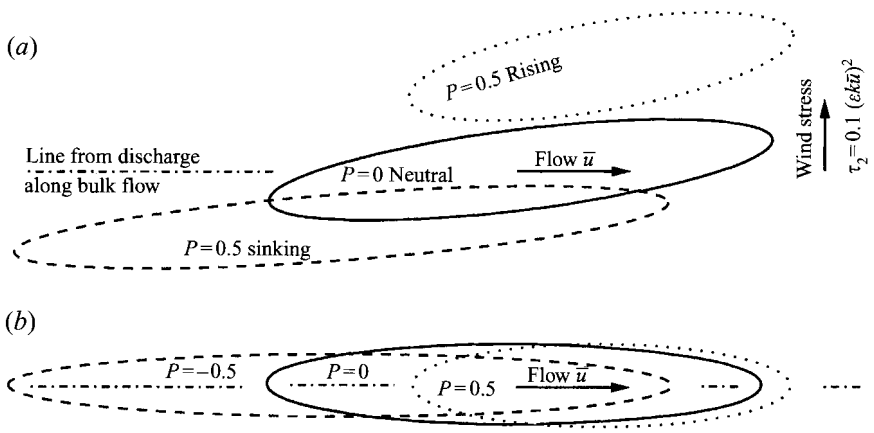

FIGURE 6. Horizontal distributions of rising particles ($P = 0.5$), solute ($P = 0$) and sinking particles ($P = -0.5$) which were released together (*a*) with and (*b*) without transverse wind.

6. Fractionation

For a sudden point discharge, the concentration distributions from the constant-coefficient equation (5.2) are exactly elliptical. If the mean current ($\bar{u}$, $\bar{v}$), wind stresses (τ_1, τ_2), and particle rise velocity W are all specified, then equations (2.4), (3.4), (5.3), (5.5*b*), (5.6) enable us to determine the wind-modified friction velocity u_*, effective horizontal velocity ($\overline{\gamma u}$, $\overline{\gamma v}$) and the shear dispersion coefficients D_{11}, D_{12}, D_{22}. Specifying the quantity discharged and the elapsed time determines the elliptical concentration contours. Figure 6 gives the standard deviation contours, (*a*) with and (*b*) without transverse wind, at a time $10h/\varepsilon k^2\bar{u}$ after discharge. To avoid overlapping between the two cases, the initial discharge positions are laterally separated (as indicated by the dot-dash lines along the bulk flow from the discharge). The mean current is assumed to be in the x-direction ($\bar{v} = 0$) and the wind is only in the y-direction ($\tau_1 = 0$). The slight change of alignment of the ellipses when there is wind can be linked to the flow at different depths. Particles of a given rise velocity W which happen to have spent more time relatively deep in the water have experienced less of the bulk flow and some of the wind-related return flow, so get displaced to negative x and y. Conversely, particles which happen to have spent more time relatively close to the surface experience more both of the bulk flow and of the wind drift, so get displaced to positive x and y. For stronger winds there would be increased lateral separation and increased transverse shear dispersion. So the ellipses would be further apart but fatter.

For a steady discharge the plume for each of the P-classes of particles is extremely elongated and can be thought of as being the superposition of the sudden discharges at all previous times. For the idealized case of a discharge at distance L from a shoreline $y = 0$ with constant depth and constant longshore current, correct to leading order in ε the shoreline concentration is

$$c_{shore} = \frac{2Q}{(2\pi)^{1/2}\sigma h\bar{u}} \exp\left\{-x\frac{\overline{\gamma\psi_0^2\alpha} + \lambda_0}{\bar{u}} - \frac{1}{2\sigma^2}\left(L + x\frac{\overline{\gamma\psi_0^2 v}}{\bar{u}}\right)^2\right\}, \tag{6.1a}$$

with

$$\sigma^2 = 2x\frac{D_{22} + \overline{\gamma\psi_0^2\kappa_2}}{\bar{u}} \tag{6.1b}$$

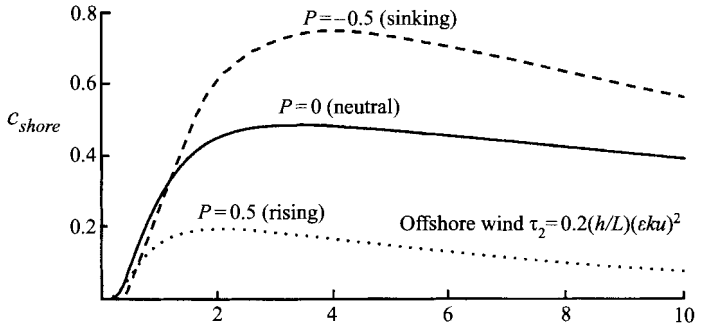

FIGURE 7. Relative concentrations on the shoreline for steady discharges of rising particles ($P = 0.5$), solute ($P = 0$) and sinking particles ($P = -0.5$) in a weak offshore wind.

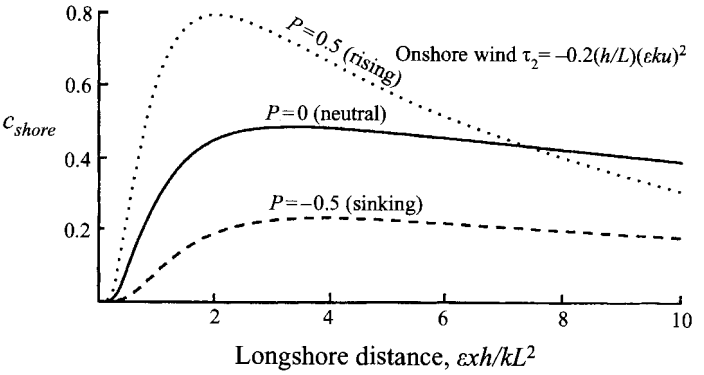

FIGURE 8. Relative concentrations on the shoreline for steady discharges of rising particles ($P = 0.5$), solute ($P = 0$) and sinking particles ($P = -0.5$) in a weak onshore wind.

(Smith 1991, equation (8.3)). Here $Q(P)$ is the source strength, x is the alongshore distance from the discharge. Figure 7 compares the shoreline concentrations when there is neither decay α in the fluid nor loss λ_0 to the bed for the particle types $P = -0.5, 0, 0.5$ when there is a weak offshore wind with strength $\tau_2 = 0.2(h/L)(\varepsilon k\bar{u})^2$. For simplicity it is assumed $h/L \ll 1, k^4$ so the wind modification to u_* is ignored and D_{22} is neglected relative to $\overline{\gamma\kappa_2}$. An offshore wind eventually brings a greater proportion of sinking material ($P = -0.5$) to the shoreline than for solutes ($P = 0$), while rising material ($P = 0.5$) either reaches the shoreline at relatively short longshore distances or is carried offshore by the wind-driven flow. Figure 8 shows that if the wind direction is reversed $\tau_2 = -0.2(h/L)(\varepsilon k\bar{u})^2$, then there is not an exact interchange of the relative concentrations for rising and of sinking particles (i.e. there is P-dependence (3.4) and (5.8) of the drift velocity and of the mixing rate). Curiously, the longshore positions of maximum concentrations are precisely the same in figures 7 and 8 (Smith 1991, equation (8.4*a*), though the proportions of particles reaching the shoreline are markedly different. In stronger winds or weaker currents, the positions and proportions for the horizontal fractionation would be more marked.

Helpful comments from the referees were gratefully appreciated. This is LOIS publication number 79 carried out under a Special Topic Award (RACS-350) from the Natural Environmental Research Council.

REFERENCES

BARTON, N. G. 1984 An asymptotic theory for dispersion of reactive contaminants in parallel flow. *J. Austral. Math. Soc.* B **25**, 287–310.

COLEMAN, N. L. 1970 Flume studies of the sediment transfer coefficient. *Water Resour. Res.* **6**, 801–809.

DYER, K. R. & SOULSBY R. L. 1988 Sand transport on the continental shelf. *Ann. Rev. Fluid Mech.* **20**, 295–324.

ELDER, J. W. 1959 The dispersion of marked fluid in turbulent shear flow. *J. Fluid Mech.* **5**, 544–560.

FISCHER, H. B. 1973 Longitudinal dispersion and turbulent mixing in open-channel flow. *Ann. Rev. Fluid Mech.* **5**, 59–78.

GIDDINGS, J. C. 1968 Nonequilibrium theory of field-flow fractionation. *J. Chem. Phys.* **49**, 81–85.

LUNGU, E. M. & MOFFATT, H. K. 1982 The effect of wall conductance on heat diffusion in duct flow. *J. Engng Maths* **16**, 121–136.

RIJN, L. C. VAN 1984 Sediment pick-up functions. *J. Hydraul. Engng ASCE* **110**, 1494–1502.

ROUSE, H. 1937 Modern conceptions of the mechanics of turbulence. *Trans. ASCE* **102**, 463–543.

SANKARASUBRAMANIAN, R. & GILL, W. N. 1973 Unsteady convective diffusion with interphase mass transfer. *Proc. R. Soc. Lond* A **333**, 115–132.

SMITH, R. 1986 Vertical drift and reaction effects upon contaminant dispersion in parallel shear flows. *J. Fluid Mech.* **165**, 425-444.

SMITH, R. 1991 Wind-augmented transport and dilution in shallow-water flows. *J. Fluid Mech.* **228**, 549–560.

SUMER, B. M. 1974 Mean velocity and longitudinal dispersion of heavy particles in turbulent open-channel flow. *J. Fluid Mech.* **65**, 11–28

TAYLOR, G. I. 1953 Dispersion of soluble matter in solvent flowing slowly through a tube. *Proc. R. Soc. Lond.* A **219**, 186–203.